

CHAPTER IV

RESULTS AND DISCUSSION

4.1 Retrofitting of the GSP5 (The Design-Data Case)

4.1.1 Data Extraction and Plant Simulation

The description of each unit and stream, and the thermal data of the GSP5, are shown in Appendix A and Table B-1. For this step, the design-data case is used to check the material balance of the process before doing the actual-data case; furthermore, it showed the scope of energy saving in the process.

The commercial simulation software, PRO/II Provision (version 5.61), with the SRK thermodynamic method, is used to simulate the heat exchanger networks (HENs) and the distillation columns. The stage numbering used the top-down procedure. The entire process consists of the demethanizer, the deethanizer, and the depropanizer. There are thirteen hot streams and six cold streams, with fourteen heat exchangers in the HENs part. The descriptions of each column simulation are explained below.

Demethanizer (3503T01): This column consists of six trays and four packed beds inside the column. However, in the simulation step, 20 trays were used to represent these packed beds that satisfy the pressure drop. The demethanizer is not a conventional column because there are many side-feed streams and a packed bed under very low temperature (the cryogenics process). This column also contains chimney trays which collect liquid from between the packed beds and function as a collector device for either feeding to a liquid distributor or liquid drawing from the column.

Deethanizer (3503T02): This column has 40 trays with feed at tray No.12 and a full reflux ratio of 1.53; the heat exchange units 3503E09 and 3503E08 are the partial condenser and reboiler, respectively.

Depropanizer (3504T01): This column consists of 98 trays and uses the heat exchange units 3504E03 and unit 3504E02 as the total condenser and reboiler, respectively. The reflux ratio is around 5.1. The feed stage is No.51. Moreover, there are two side draws at tray No.23 (LPG) and No.89 (i-pentane).

The process flow sheet of the GSP5 is represented in Figure B-2. To ensure the PPO/II-simulation of the GSP5, Table 4.1 shows the accuracy parameters of the process simulation in the design-data case.

Table 4.1 Accuracy parameters of process simulation by Pro/II compared to the design data

| Parameter | Simulation Error Value |
|------------------------------------|------------------------|
| Composition | ± 0.05 |
| Flow rate (KGMOL/HR) | $\pm 5 \%$ |
| Temperature ($^{\circ}\text{C}$) | ± 3 |
| Pressure (BAR_G) | ± 2 |

4.1.2 Heat Exchanger Networks of the Background Process

The GSP5 is the low temperature process having fourteen heat exchange units between hot and cold process streams. From the data extraction of the design-data case, the grid diagram is performed as shown in Figure 4.1. Pinch analysis was applied to figure out the minimum approach temperature (ΔT_{\min}) of the process. This involves using the problem table algorithm (PTA) to obtain the utility requirements for various ΔT_{\min} and a trial-and-error procedure to ascertain the ΔT_{\min} for the design utility level. All process stream calculations are given in Table 4.2.

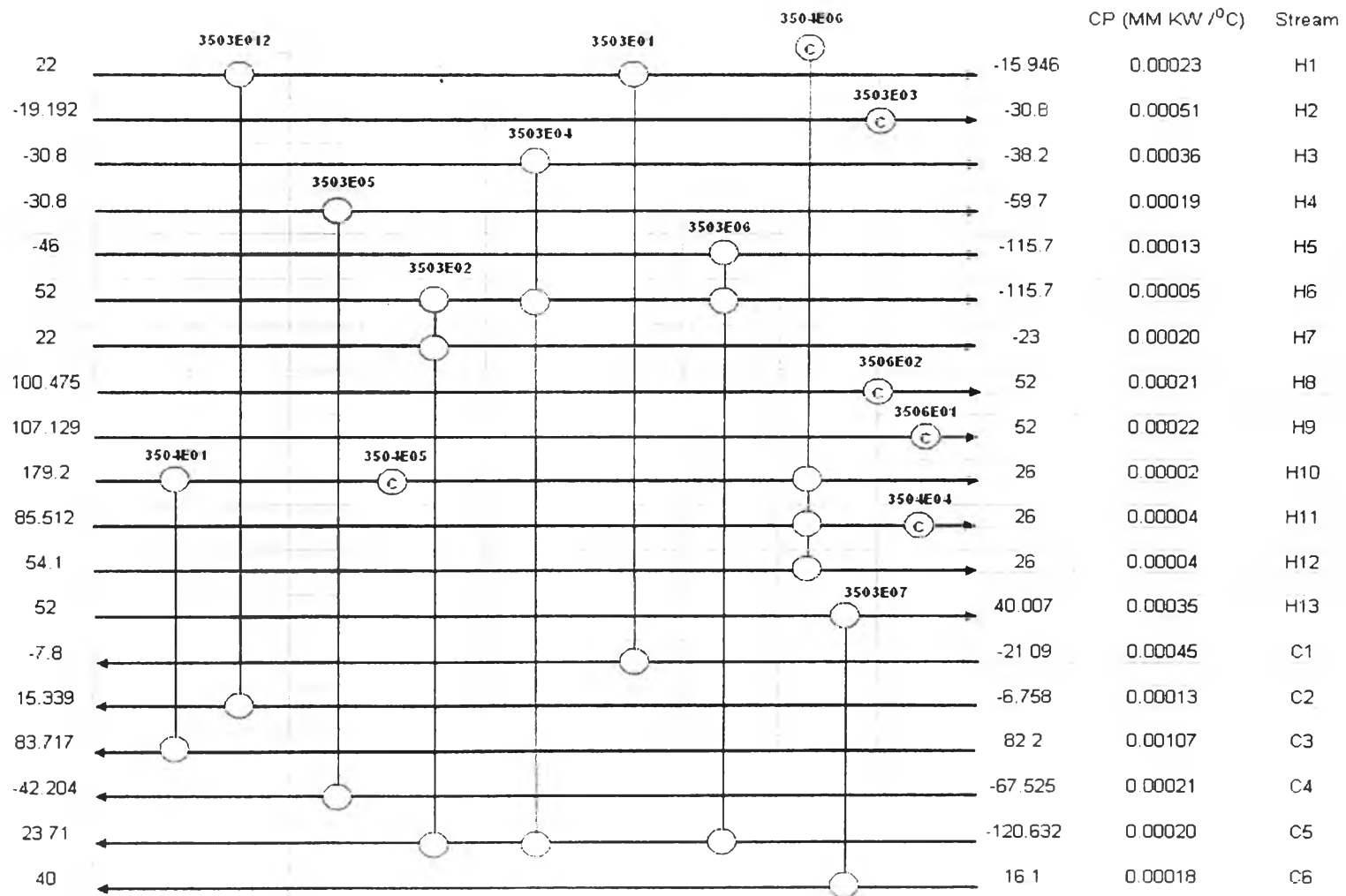


Figure 4.1 Grid diagram of the design-data case.

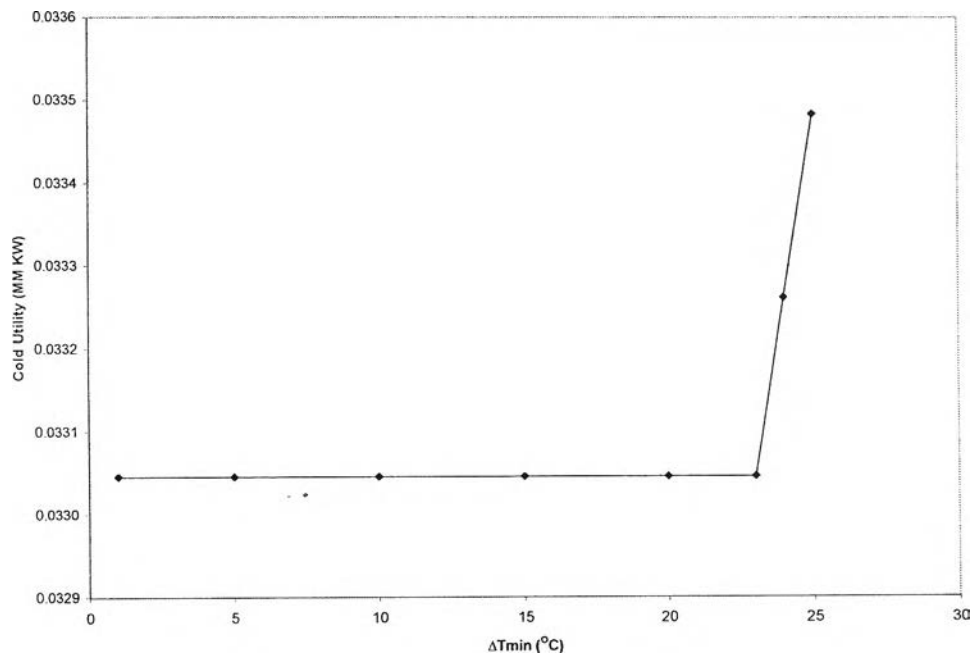
Table 4.2 Process stream data of the design-data case

| Type of Stream | Flow Rate MM KG/H | T _{in} °C | T _{out} °C | CP MM KW/°C | Heat Duty MM KW |
|----------------|----------------------|-----------------------|------------------------|----------------|--------------------|
| H1 | 0.240134 | 22 | -15.946 | 0.000233 | 0.0089 |
| H2 | 0.442236 | -19.192 | -30.8 | 0.000514 | 0.0060 |
| H3 | 0.298952 | -30.8 | -38.2 | 0.000360 | 0.0027 |
| H4 | 0.143285 | -30.8 | -59.7 | 0.000186 | 0.0054 |
| H5 | 0.126543 | -46 | -115.7 | 0.000133 | 0.0093 |
| H6 | 0.037925 | 52 | -115.7 | 0.000047 | 0.0078 |
| H7 | 0.202102 | 22 | -23 | 0.000202 | 0.0091 |
| H8 | 0.314972 | 100.475 | 52 | 0.000212 | 0.0103 |
| H9 | 0.314972 | 107.129 | 52 | 0.000221 | 0.0122 |
| H10 | 0.021162 | 179.2 | 26 | 0.000016 | 0.0025 |
| H11 | 0.05359 | 85.512 | 26 | 0.000043 | 0.0026 |
| H12 | 0.044823 | 54.1 | 26 | 0.000040 | 0.0011 |
| H13 | 0.384401 | 52 | 40.007 | 0.000354 | 0.0043 |
| C1 | 0.202301 | -21.09 | -7.8 | 0.000447 | 0.0059 |
| C2 | 0.17086 | -6.758 | 15.339 | 0.000132 | 0.0029 |
| C3 | 0.119576 | 82.2 | 83.717 | 0.001071 | 0.0016 |
| C4 | 0.199541 | -67.525 | -42.204 | 0.000213 | 0.0054 |
| C5 | 0.314999 | -120.632 | 23.71 | 0.000200 | 0.0288 |
| C6 | 0.169529 | 16.1 | 40 | 0.000178 | 0.0043 |

The GSP5 is an unpinch process with ΔT_{\min} lower than the threshold ΔT_{\min} of 23°C, as listed in Table 4.3. There is only a cold utility of air and refrigerant-propane consumptions of 0.03305 MM KW. A condenser and a reboiler of the deethanizer (heat exchange units 3503E08 and 3503E09AB) and a condenser and a reboiler of the depropanizer (heat exchange units 3504E02 and 3504E03) were omitted when doing HENs of the background process because their duties were used and modeled in the columns. Figures 4.2(a) and 4.2(b) present the minimum energy requirement of each ΔT_{\min} . Querzoli and Hoadley (2002) applied utility pinch to find the ΔT_{\min} for the unpinch problem. In this case, air cooled heat exchangers are applied to match the energy consumption, as summarized in Table 4.4. The reason for not using refrigerant-propane heat exchangers is due to the phase change problem. The grand composite curves (GCCs) of the background process for various ΔT_{\min} in the range of threshold problem are shown in Figure 4.3.

Table 4.3 Utility summary for various ΔT_{\min}

| ΔT_{\min} (°C) | Cold Utility (MM KW) | Hot Utility (MM KW) |
|------------------------|----------------------|---------------------|
| 1 | 0.03305 | 0 |
| 5 | 0.03305 | 0 |
| 10 | 0.03305 | 0 |
| 15 | 0.03305 | 0 |
| 20 | 0.03305 | 0 |
| 23 | 0.03305 | 0 |
| 24 | 0.03326 | 0.00022 |
| 25 | 0.03348 | 0.00044 |

**Figure 4.2(a)** Relationship between ΔT_{\min} and cold utility with the threshold $\Delta T_{\min} = 23^\circ\text{C}$.

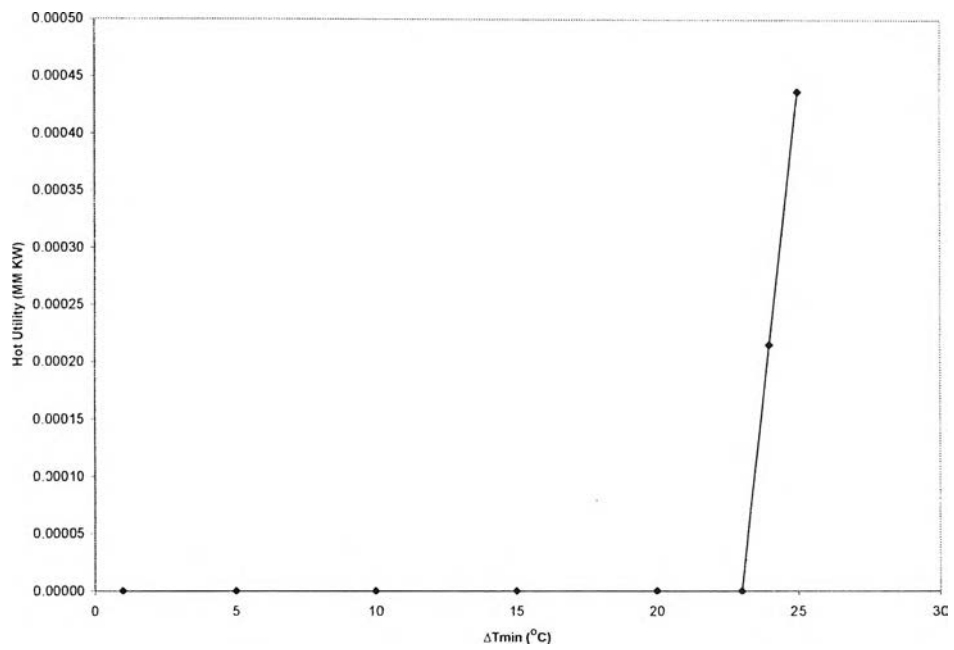


Figure 4.2(b) Relationship between ΔT_{\min} and hot utility with the threshold $\Delta T_{\min}=23^{\circ}\text{C}$.

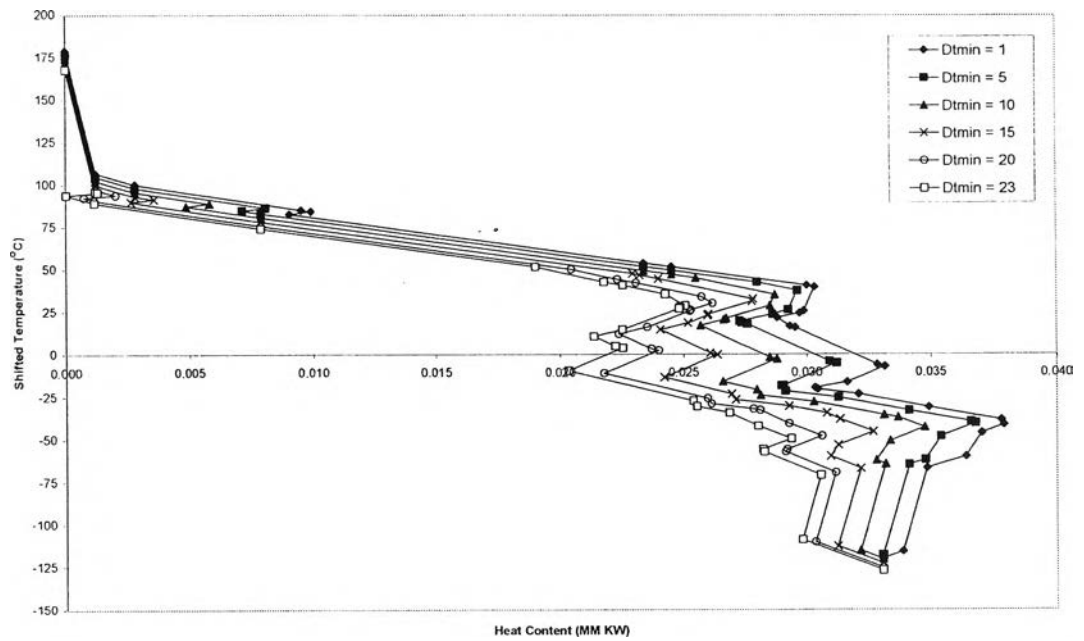
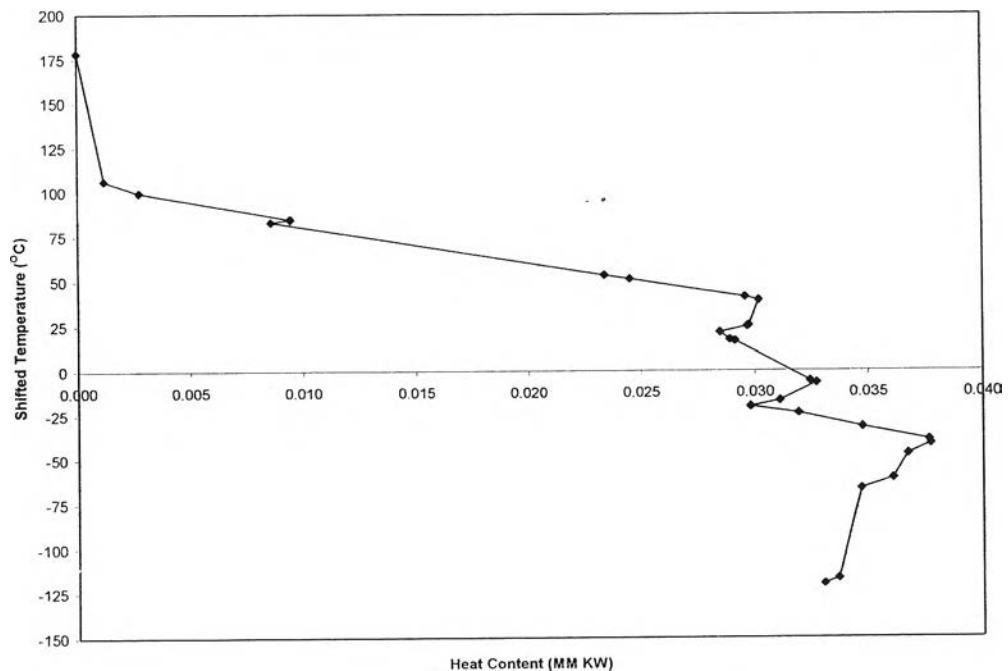


Figure 4.3 GCCs for various ΔT_{\min} in the range of threshold problem.

Table 4.4 Cold utility con for ΔT_{\min} in the range of 1 to 15°C

| ΔT_{\min} (°C) | Cold Utility (MM KW) | |
|----------------------------------|----------------------|----------------|
| | Air | Refrigerant-C3 |
| 1 | 0.02500 | 0.00806 |
| 2 | 0.02450 | 0.00856 |
| 5 | 0.02340 | 0.00966 |
| 10 | 0.02050 | 0.01256 |
| 15 | 0.01780 | 0.01526 |
| The design-data case (1.85°C) | 0.02457 | 0.00848 |

The ΔT_{\min} of the process for the design-data case is 1.85°C. Figures 4.4 and B-1 show the GCC and the PTA of the design-data case. From the observing, the modifications of heat exchanger networks can not be done because the process has no process pinch (no pinch point), resulting in no heat transfer across the pinch and no wrong position utility.

**Figure 4.4** GCC of the design-data case ($\Delta T_{\min} = 1.85^\circ\text{C}$).

4.1.3 Distillation Column Targeting

This section starts with generating the column grand composite curve (CGCC) of each distillation column separately by using a converged simulation of each column based on top-down and bottom-up procedures. The selection of key components is the important thing for column targeting. In this work, the key components are selected based on their boiling points (shown in Table 4.5), and the column composition profile on a stage-by-stage basis.

The CGCC provides a thermal profile for a distillation column and identifies appropriate targets for the column modifications. Both reboiler and condenser duties of each column in the design-data case are summarized in Table 4.6. Furthermore, the errors of results came from the calculation model and the choosing of the key components.

Table 4.5 Boiling points of components (PRO/II Provision)

| Component | Boiling Point (°C) |
|-------------------|--------------------|
| N ₂ | -195.8 |
| CO ₂ | -78.48 |
| METHANE | -161.49 |
| ETHANE | -88.63 |
| PROPANE | -42.07 |
| IBUTANE | -11.73 |
| BUTANE | -0.5 |
| IPENTANE | 27.85 |
| PENTANE | 36.07 |
| HEXANE | 68.74 |
| HEPTANE | 98.43 |
| OCTANE | 125.67 |
| NONANE | 150.8 |
| H ₂ S | -60.34 |
| COS | -50.2 |
| H ₂ O | 100 |
| TEG | 288.35 |
| CH ₄ S | 5.96 |
| ETSH | 35.05 |
| PN1THIOL | 126.65 |
| BU1THIOL | 98.46 |

Table 4.6 Reboiler and condenser duties of each column from PRO/II-simulator and excel CGCC

| Distillation Column | Condenser Duty (MM KW) | | | Reboiler Duty (MM KW) | | |
|---------------------|------------------------|---------------|-----------|-----------------------|---------------|-----------|
| | Simulation by Pro/II | CGCC by Excel | Error (%) | Simulation by Pro/II | CGCC by Excel | Error (%) |
| Demethanizer | | | | | | |
| Deethanizer | 0.01088 | 0.01088 | 0 | 0.0160 | 0.0175 | 9.375 |
| Depropanizer | 0.01913 | 0.01913 | 0 | 0.0164 | 0.0164 | 0 |

Demethanizer (3503T01): Here, there is no reason to generate the CGCC because the demethanizer has neither condenser nor reboiler loads; furthermore, this column is a non-conventional type, having many feed trays and causing more accumulative errors in the method (Santanu Bandyopadhyay, Ranjan K. Malik, and Uday V. Shenoy, 1998). Figure 4.5 shows the demethanizer column composition profile.

Deethanizer (3503T02): The column composition profile in Figure 4.6(a) used nitrogen, methane, ethane, CO₂, H₂S, and COS as the light key components. The CGCC of the deethanizer, shown in Figure 4.6(b), gives only one pinch point near the feed position around tray temperature 36.7°C (The design feed stage and temperature are 12 and 36°C, respectively).

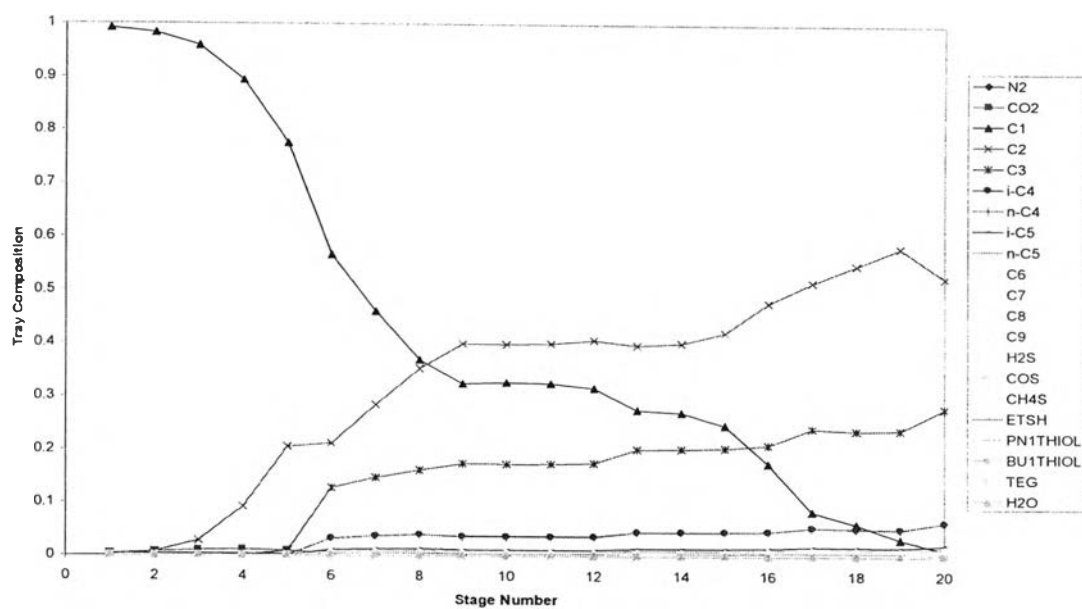


Figure 4.5 Demethanizer column composition profile (design-data case).

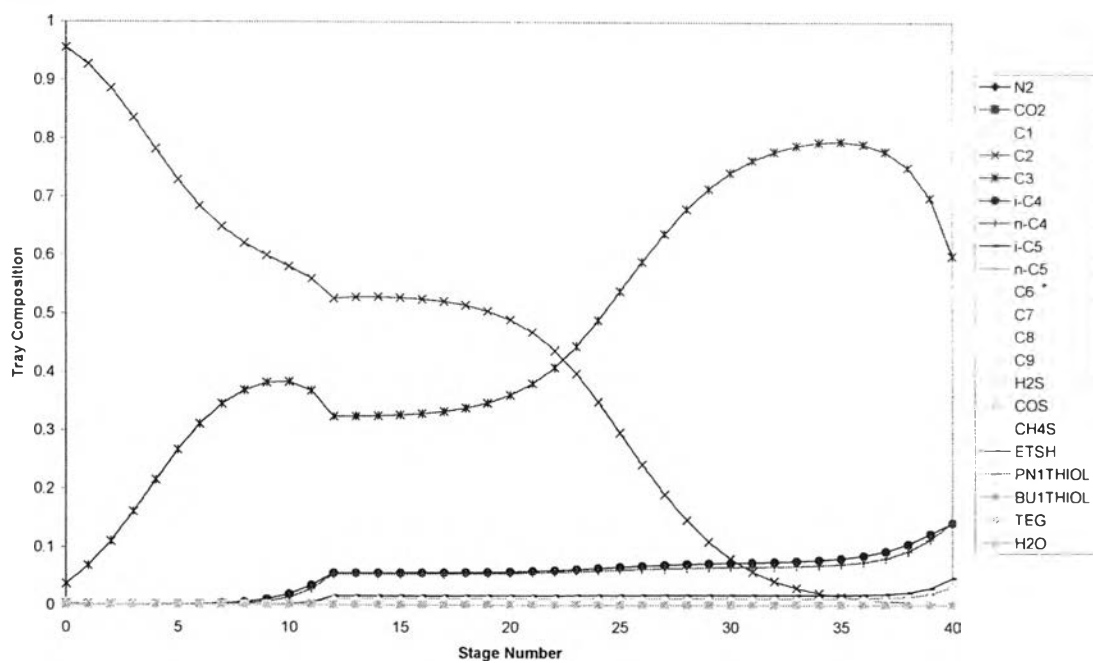


Figure 4.6(a) Deethanizer column composition profile (design-data case).

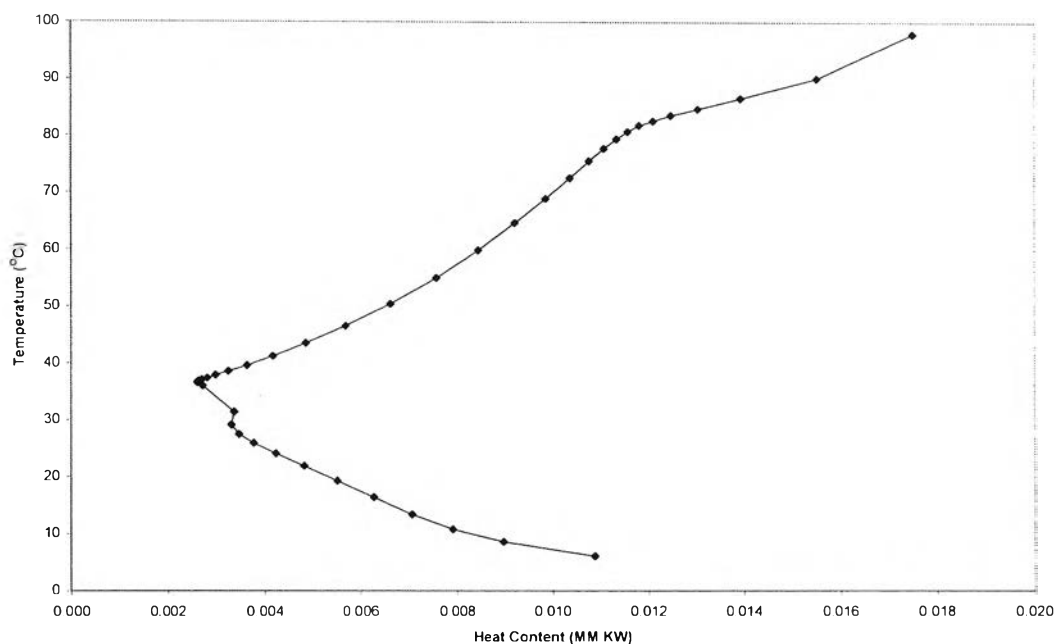


Figure 4.6(b) CGCC of the deethanizer (design-data case).

Depropanizer (3504T01): Before generating the CGCC, the key compositions had to be specified first. The depropanizer column composition profile is used for specifying the key component, as shown in Figure 4.7(a). As a result, the light key components are nitrogen, methane, ethane, CO₂, H₂S, COS, and propane. The CGCC of the depropanizer in Figure 4.7(b) had one pinch point around tray temperature 87.6°C, which is quite near the position of the feed stage (The design feed stage and temperature are 51 and 92.6°C, respectively).

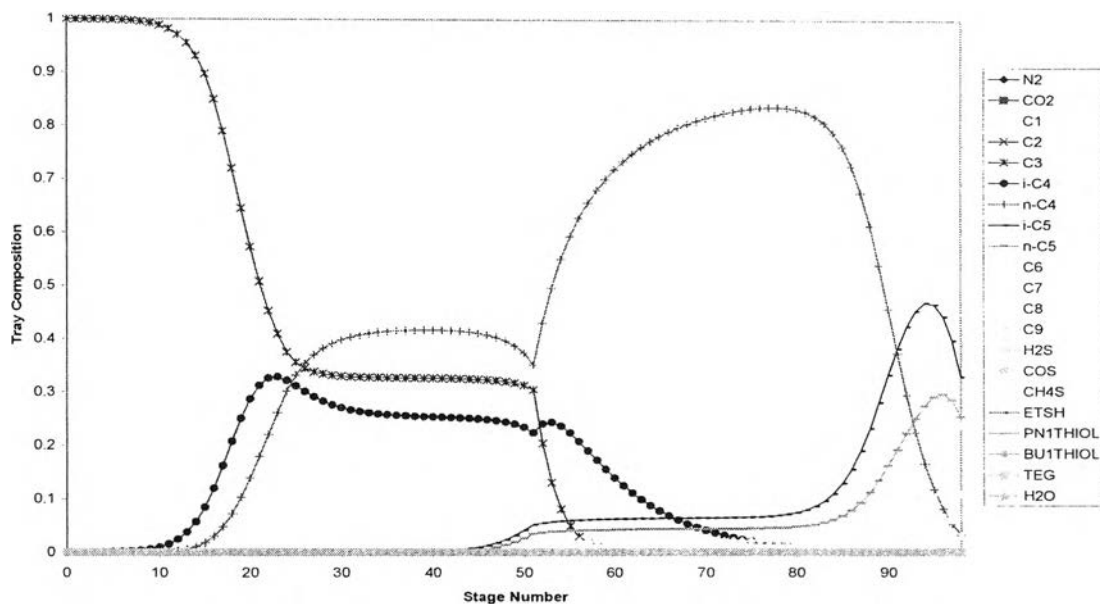


Figure 4.7(a) Depropanizer column composition profile (design-data case).

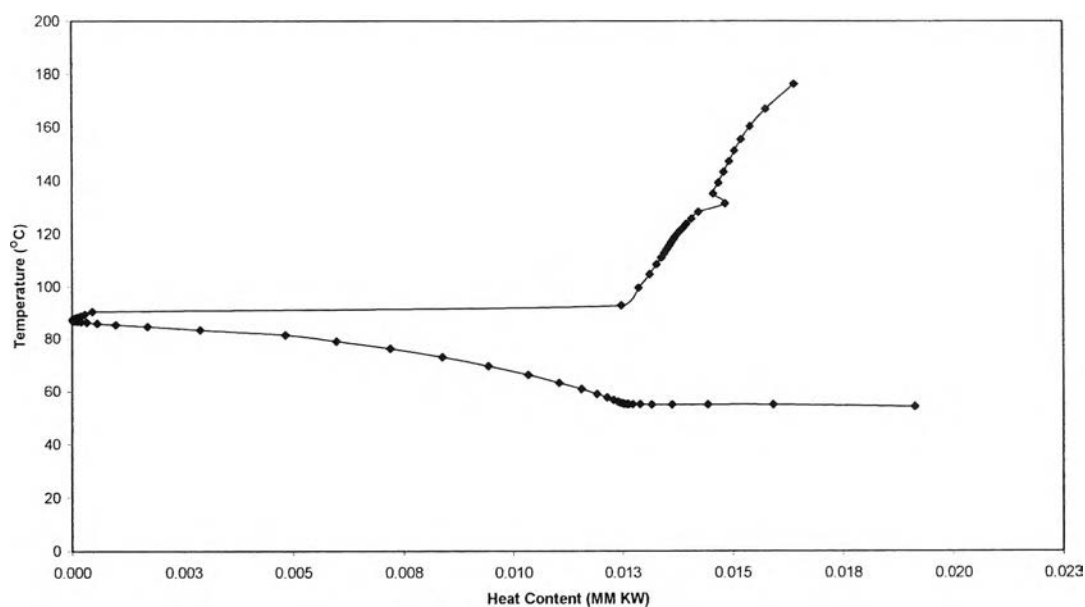


Figure 4.7(b) CGCC of the depropanizer (design-data case).

4.1.3.1 Stand-Alone Column Modifications

Demethanizer (3503T01): There is no improvement from the CGCC construction. The alternative for improving the demethanizer is to reduce the shaftwork consumption through the refrigeration system because the demethanizer

section is a very low temperature process (the cryogenics process) dominated by the shaftwork consumption of a compressor in the refrigeration system.

Deethanizer (3503T02): The CGCC from Figure 4.6(b) shows a gap between the pinch point and the temperature axis, indicating the scope of reflux modification. This gap may be reduced by lowering the reflux ratio, resulting in a reduction in both reboiler and condenser loads. It must be noted that, in order to make a judicious choice for reflux ratio, the increase in the capital cost due to the increase in the number of stages and complexity of modification should be traded-off against the saving in energy cost. Moreover, plotting stage number versus enthalpy (Figure 4.8) shows no sharp change in enthalpy near the feed position, which implies no scope for the feed condition.

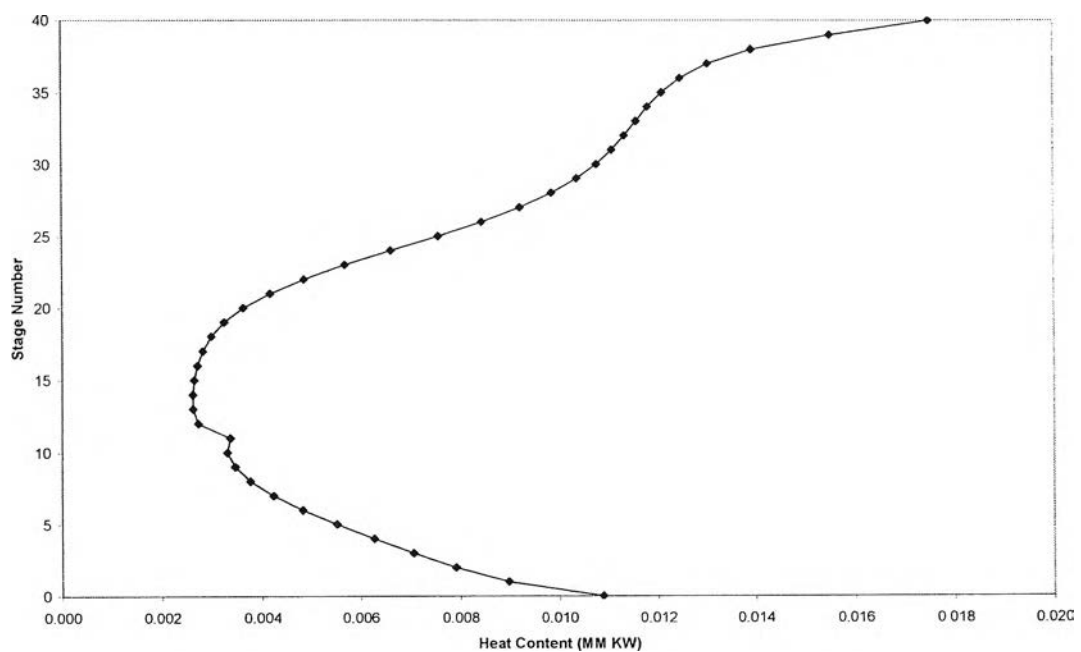


Figure 4.8 Stages versus enthalpy of the deethanizer (design-data case).

Depropanizer (3504T01): There is no scope of reflux modification from the CGCC in Figure 4.7(b); however, Figure 4.9 indicates the scope of feed preheating above feed position.

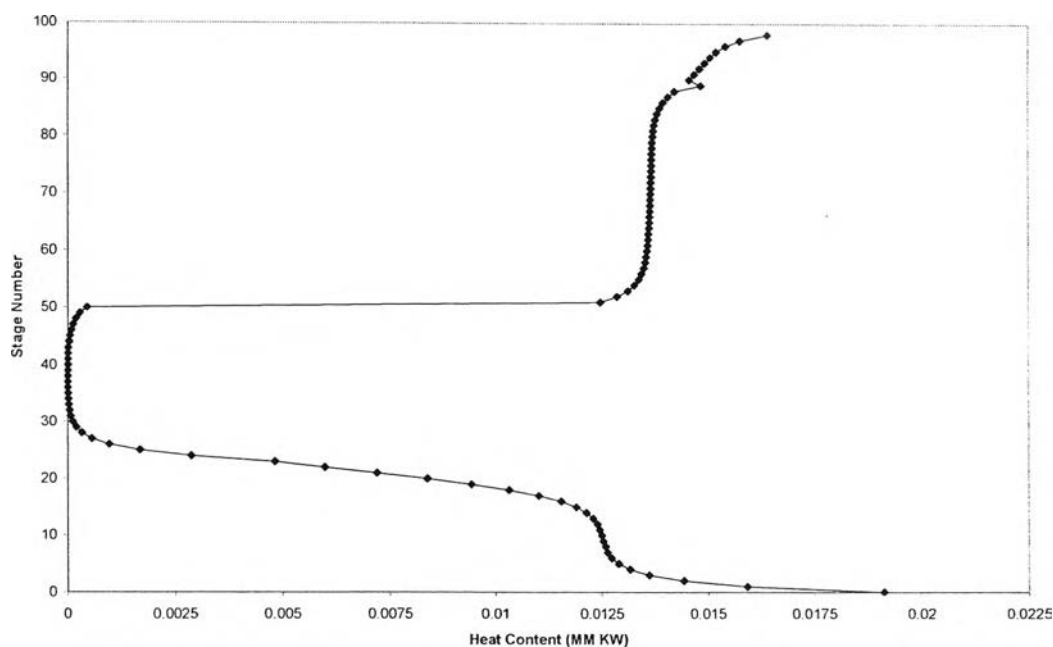


Figure 4.9 Stages versus enthalpy of the depropanizer (design-data case).

4.1.4 Process Heat Integration

Process heat integration is a further improvement of the overall energy efficiency of the process by the appropriate integration of the column with the background process. In this case, this technique is only done for the deethanizer and the depropanizer, starting with plotting the CGCC of both the deethanizer and the depropanizer in reverse direction superimposed on the GCC of the background process, as shown in Figure 4.10.

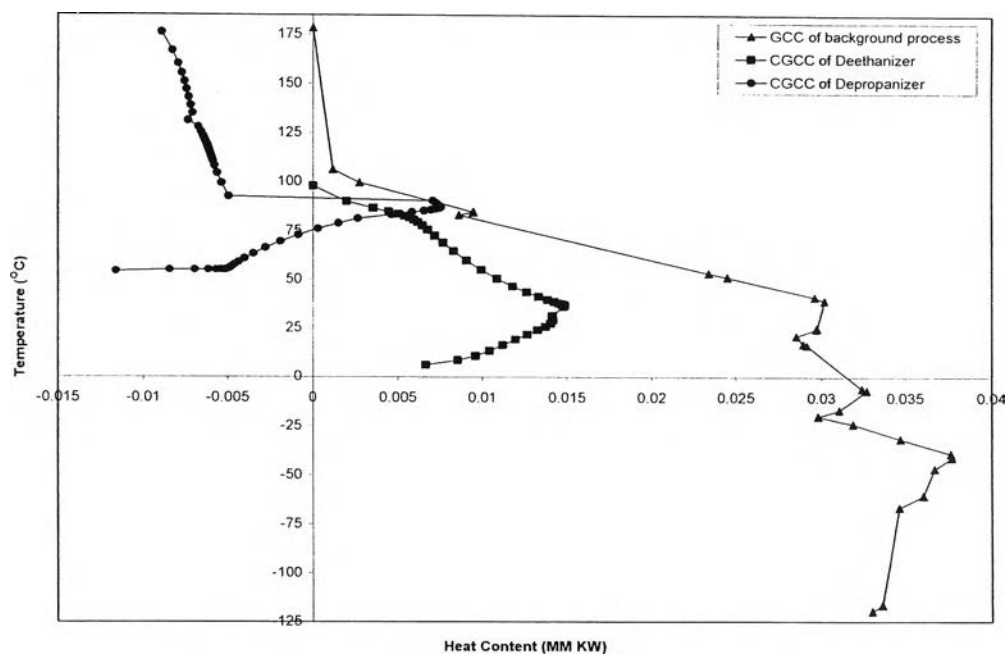


Figure 4.10 Process heat integration of the design-data case.

4.1.4.1 Process Heat Integration between the Background Process and the Deethanizer

Figure 4.10 implies an energy saving from the process heat integration between the heat exchanger network of the background process and the deethanizer by integrating a hot process stream which has a temperature above 71°C. with a new side reboiler on the deethanizer around at a tray temperature of 36.7-97.9°C because the reboiler of the deethanizer can get heat from a hot process stream of the background process.

4.1.4.2 Process Heat Integration between the Background Process and the Depropanizer

Similar to for the deethanizer, Figure 4.10 also clearly indicates the scope of energy saving from the process heat integration by integrating a hot process stream (above 90.5°C) with a new side reboiler of the deethanizer around a tray temperature of 87.1-92.6°C.

4.2 Retrofitting of the GSP5 (The Actual-Data Case)

4.2.1 Data Extraction and Plant Simulation

After collecting the actual data of the GSP5, the molar composition and some specifications of columns were changed from the design-data case; furthermore, some data from the design-data case were used to do the actual-data case simulation. The GSP5 has a capacity of around 530 MMSCFD, which produces methane, ethane, propane, LPG, and NGL as products. Tables 4.7 and 4.8 show the constrained parameters to assure the reliability of the process data and the product specifications of the GSP5. The thermal data of streams and the GSP5 flow sheet in the actual-data case are represented in Table C-1 and Figure C-2, respectively.

Table 4.7 Accuracy parameters of process simulation

| Parameter | Simulation Error Value |
|------------------------------------|------------------------|
| Composition | ± 0.05 |
| Flow rate (KGMOL/HR) | $\pm 10\%$ |
| Temperature ($^{\circ}\text{C}$) | ± 3 |
| Pressure (BAR_G) | ± 4 |

Table 4.8 Product specifications of the GSP5

| GSP5 Product | Impurity Component | Maximum % Mole Limitation |
|--------------------|--------------------|---------------------------|
| Ethane to ETU | C1 | 1.9 |
| | C3 | 2.5 |
| | CO ₂ | 3.0 |
| Propane to Storage | C2 | 2.0 |
| | C4 | 0.01 |
| LPG to Storage | C2 | 2.0 |
| | n-C5 | 1.9 |
| NGL to Storage | Max RVP~ 14 PSIG | |

4.2.2 Heat Exchanger Networks of the Background Process

From the data extraction of the actual-data case, the grid diagram of the current heat exchanger networks is performed as shown in Figure 4.11 and all of the process stream calculations are summarized in Table 4.9.

Table 4.9 Process stream data of the existing process

| Type of Stream | Flow Rate MM KG/H | T _{in} °C | T _{out} °C | CP MM KW/°C | Heat Duty MM KW |
|----------------|----------------------|-----------------------|------------------------|----------------|--------------------|
| H1 | 0.255191 | 19.03 | -1.797 | 0.000229 | 0.0048 |
| H2 | 0.431796 | -11.388 | -30.8 | 0.000504 | 0.0098 |
| H3 | 0.291894 | -30.8 | -39.6 | 0.000345 | 0.0030 |
| H4 | 0.139902 | -30.8 | -55.6 | 0.000179 | 0.0044 |
| H5 | 0.123991 | -47.2 | -116.7 | 0.000131 | 0.0091 |
| H6 | 0.037179 | 43.594 | -116.8 | 0.000047 | 0.0075 |
| H7 | 0.176605 | 19.03 | -24.2 | 0.000178 | 0.0077 |
| H8 | 0.31089 | 98.84 | 41.4 | 0.000208 | 0.0119 |
| H9 | 0.31089 | 100.057 | 43.8 | 0.000217 | 0.0122 |
| H10 | 0.009385 | 171.809 | 17.9 | 0.000007 | 0.0011 |
| H11 | 0.06551 | 72.678 | 18.51 | 0.000053 | 0.0029 |
| H12 | 0.017967 | 54 | 19.02 | 0.000016 | 0.0005 |
| H13 | 0.226041 | 52 | 33.795 | 0.000204 | 0.0037 |
| C1 | 0.093317 | -10.813 | -4.5 | 0.000391 | 0.0025 |
| C2 | 0.160637 | -3.57 | 14.56 | 0.000126 | 0.0023 |
| C3 | 0.092934 | 78.098 | 78.882 | 0.000935 | 0.0007 |
| C4 | 0.149159 | -60.723 | -35.361 | 0.000175 | 0.0044 |
| C5 | 0.309723 | -120.645 | 18.878 | 0.000196 | 0.0273 |
| C6 | 0.160637 | 14.467 | 37.7 | 0.000160 | 0.0037 |

The GSP5 is an unpinch process with ΔT_{\min} lower than the threshold ΔT_{\min} of 21°C. There is still no hot utility usage, yet there is an existing cold utility of air and refrigerant-propane consumption of 0.0377 MM KW. The existing process has the ΔT_{\min} of around 1.06°C. Figures 4.12(a) and 4.12(b) present the minimum energy requirements of each ΔT_{\min} . The GCCs of the background process for various ΔT_{\min} in the range of threshold problem and the GCC of the existing process are shown in Figures 4.13 and 4.14, respectively. The PTA of the existing process is illustrated in Figure C-1. From the observing, the modifications of heat exchanger

networks can not be done because the GSP5 has no process pinch (no pinch point), resulting in no heat transfer across the pinch and no wrong position utility.

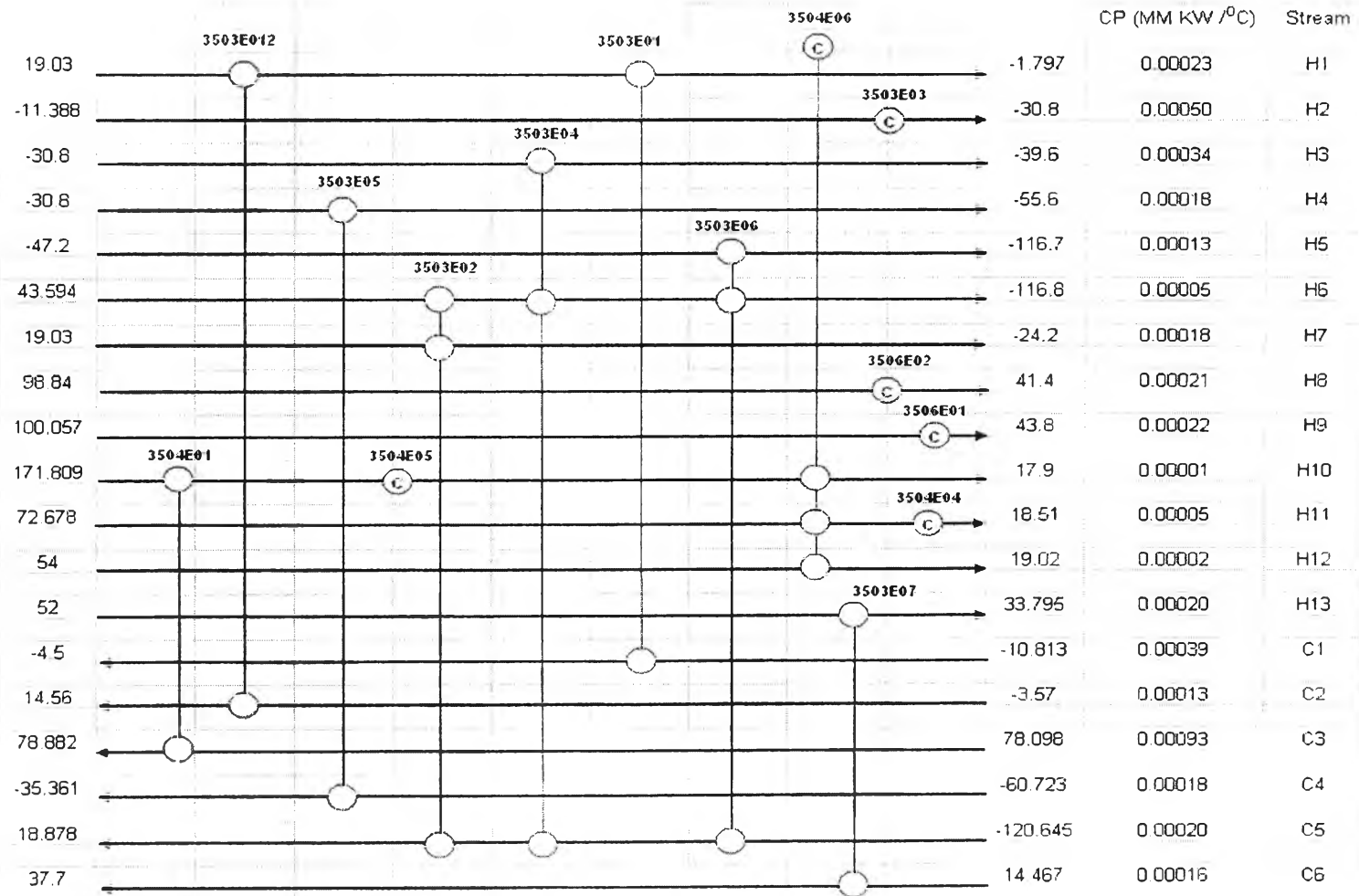


Figure 4.11 Grid diagram of the existing process.

Table 4.10 Utility summary for various ΔT_{\min}

| ΔT_{\min} (°C) | Cold Utility (MM KW) | Hot Utility (MM KW) |
|------------------------|----------------------|---------------------|
| 1 | 0.0377 | 0 |
| 5 | 0.0377 | 0 |
| 10 | 0.0377 | 0 |
| 15 | 0.0377 | 0 |
| 20 | 0.0377 | 0 |
| 21 | 0.0377 | 0 |
| 22 | 0.0378 | 0.0001702 |

Table 4.11 Cold utility for ΔT_{\min} in the range of 1 to 15°C

| ΔT_{\min} (°C) | Cold Utility (MM KW) | |
|----------------------------------|----------------------|----------------|
| | Air | Refrigerant-C3 |
| 1 | 0.02595 | 0.01176 |
| 2 | 0.02530 | 0.01241 |
| 5 | 0.02310 | 0.01461 |
| 10 | 0.02010 | 0.01761 |
| 15 | 0.01760 | 0.02011 |
| The existing process (1.06°C) | 0.02591 | 0.01180 |

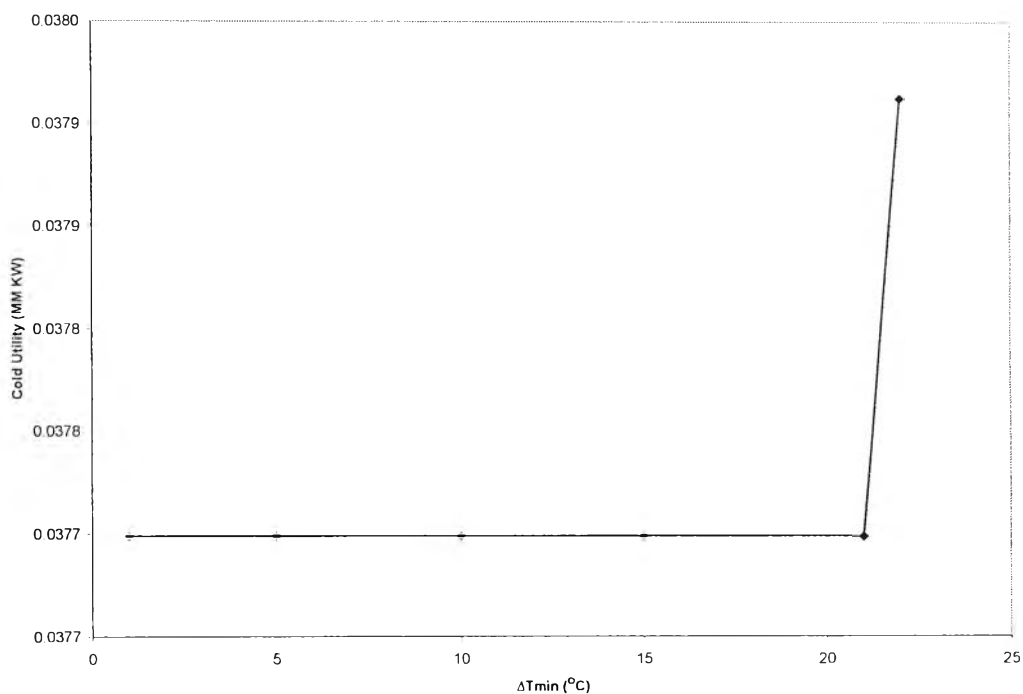


Figure 4.12(a) Relationship between ΔT_{\min} and cold utility with the threshold $\Delta T_{\min}=21^{\circ}\text{C}$.

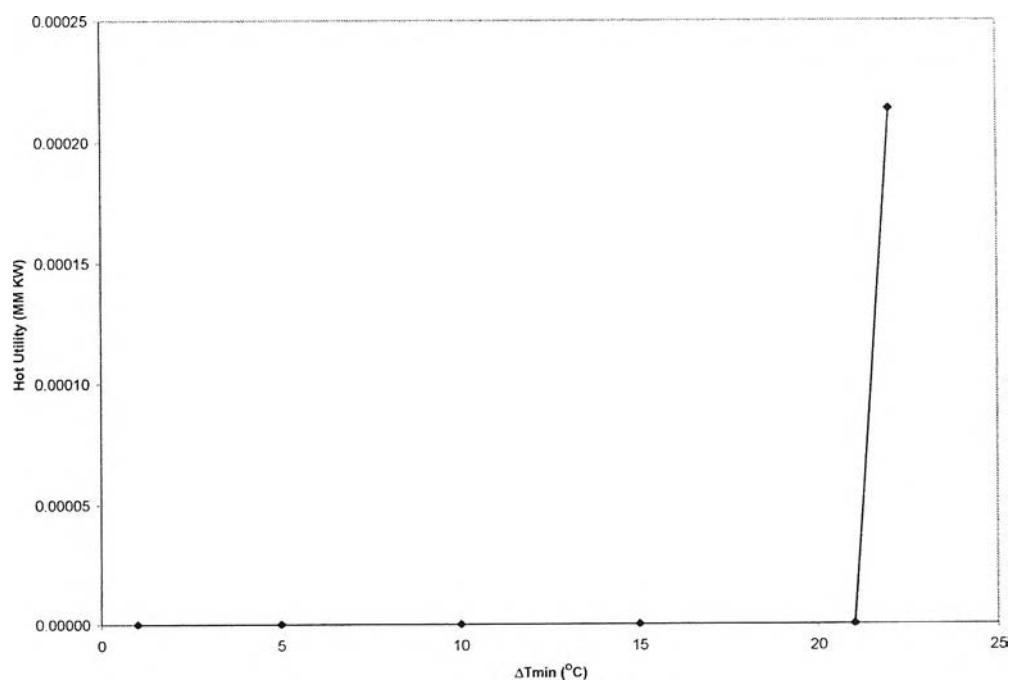


Figure 4.12(b) Relationship between ΔT_{\min} and hot utility with the threshold $\Delta T_{\min}=21^{\circ}\text{C}$.

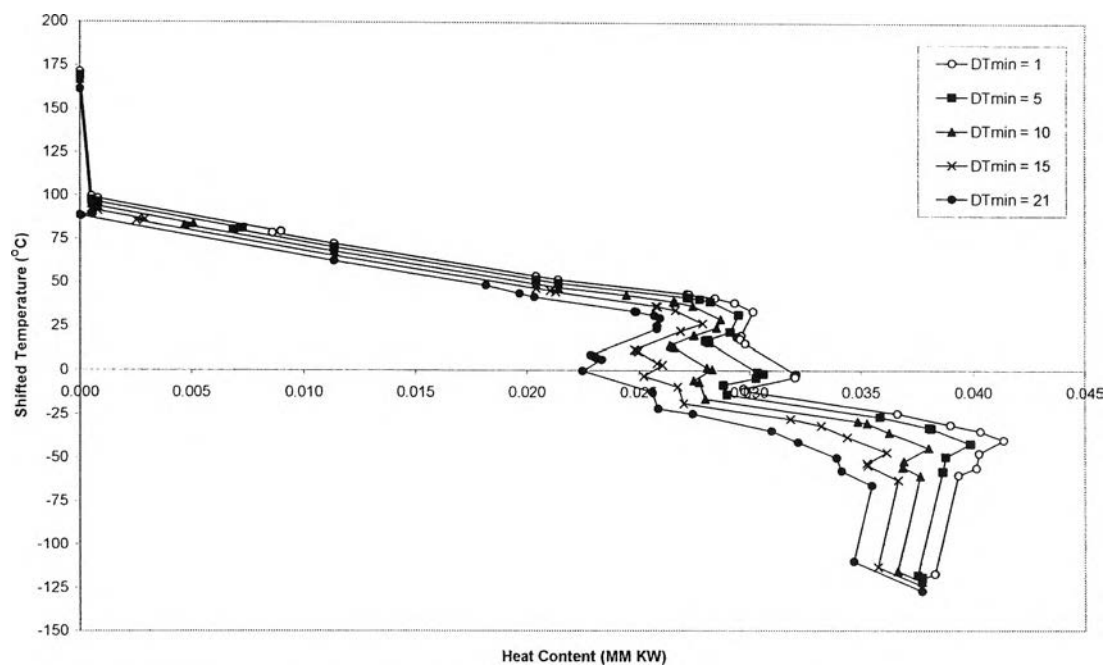


Figure 4.13 GCCs for various ΔT_{\min} in the range of threshold problem.

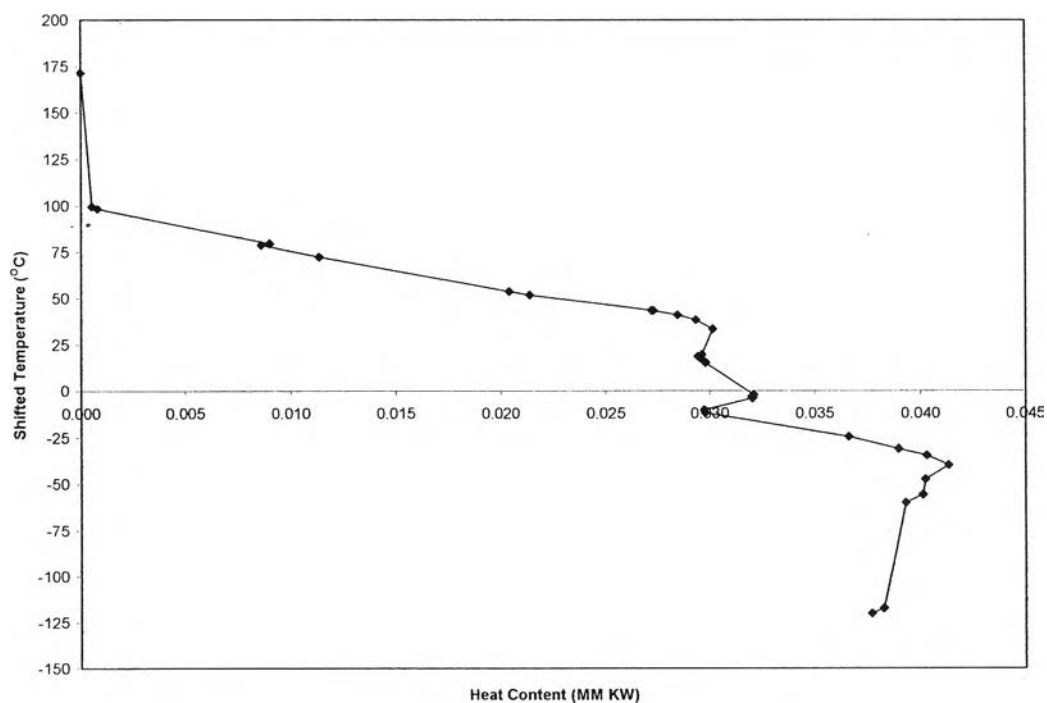


Figure 4.14 GCC of the existing process ($\Delta T_{\min} = 1.06^{\circ}\text{C}$).

4.2.3 Distillation Column Targeting

Similar to the design-data case, the CGCC of each fractionation column is generated by using a converged simulation of each column based on the top-down and bottom-up procedures. Both reboiler and condenser duties of each column in the actual-data case are summarized in Table 4.12.

Table 4.12 Reboiler and condenser duties of each column from PRO/II-simulator and excel CGCC

| Distillation column | Condenser Duty (MM KW) | | | Reboiler Duty (MM KW) | | |
|---------------------|------------------------|---------------|-----------|-----------------------|---------------|-----------|
| | Simulation by Pro/II | CGCC by Excel | Error (%) | Simulation by Pro/II | CGCC by Excel | Error (%) |
| Demethanizer | | | | 0.0048 | | |
| Deethanizer | 0.009911 | 0.009911 | 0 | 0.0165 | 0.0174 | 5.74 |
| Depropanizer | 0.01127 | 0.01053 | 6.59 | 0.0076 | 0.0076 | 0 |

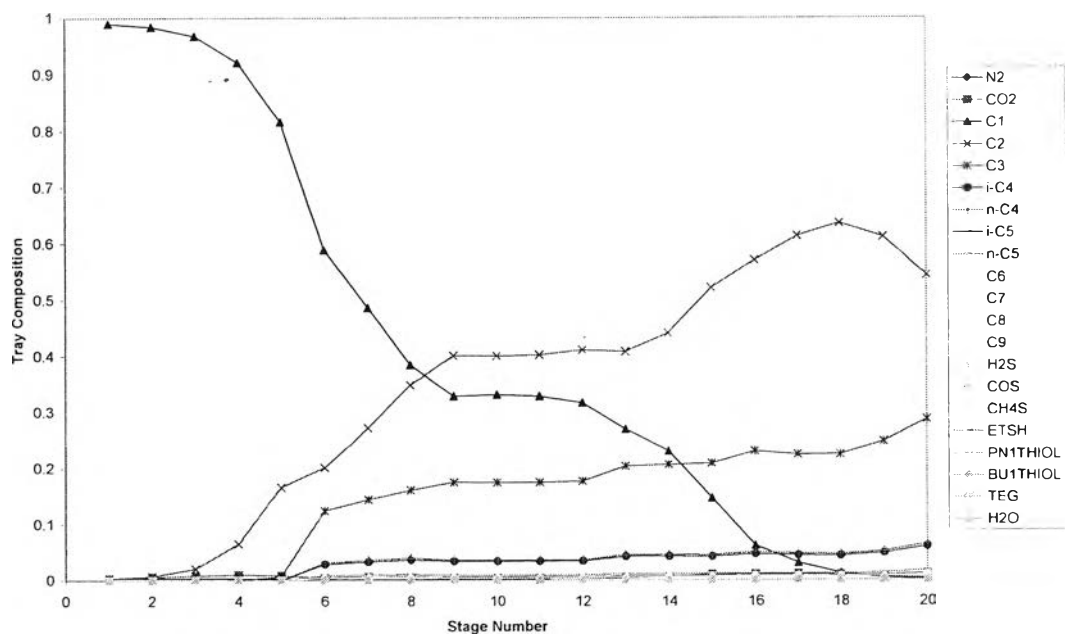


Figure 4.15 Demethanizer column composition profile (actual-data case).

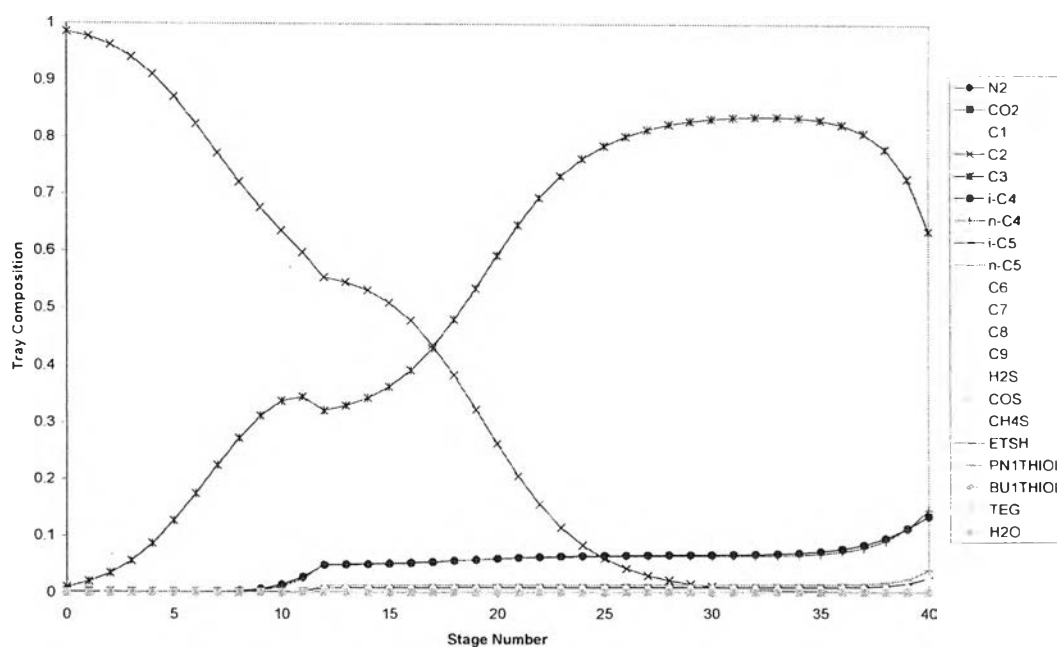


Figure 4.16(a) Deethanizer column composition profile (actual-data case).

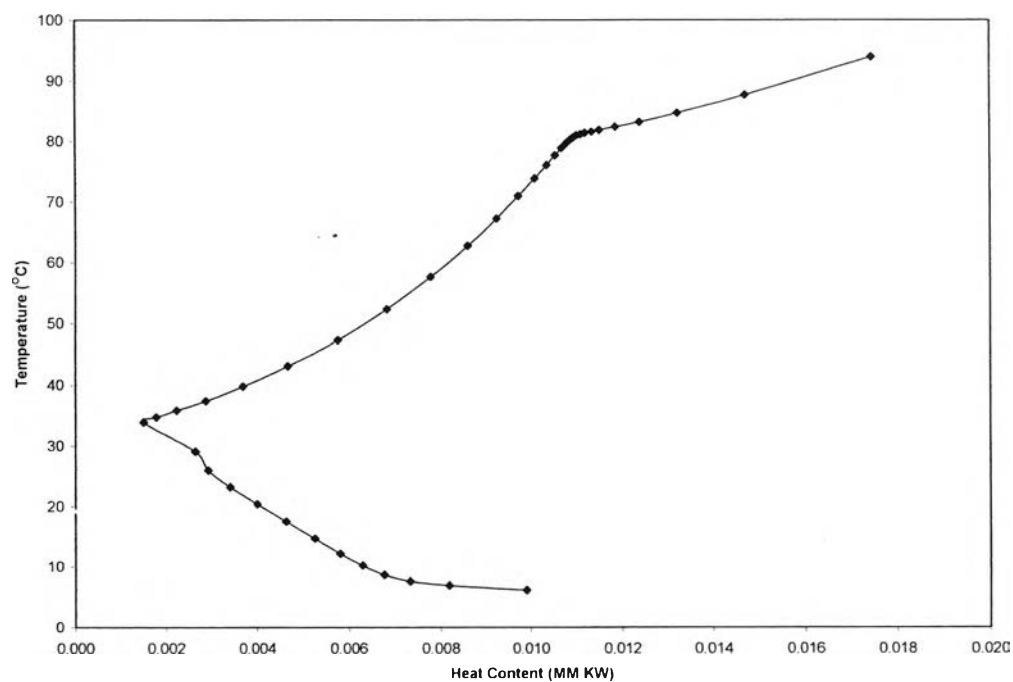


Figure 4.16(b) CGCC of the deethanizer (actual-data case).

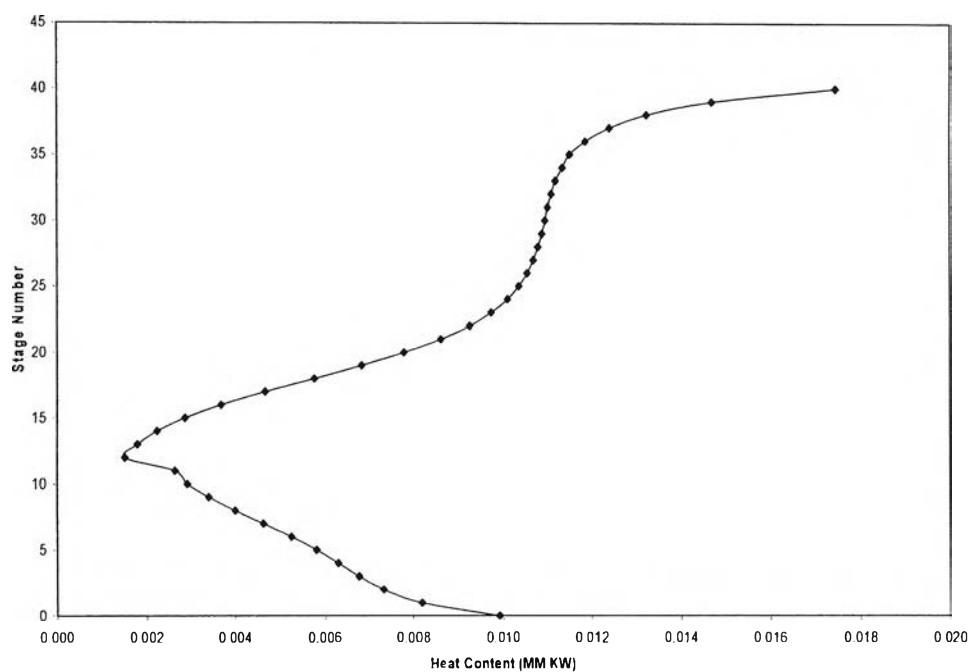


Figure 4.16(c) Stages versus enthalpy of the deethanizer (actual-data case).

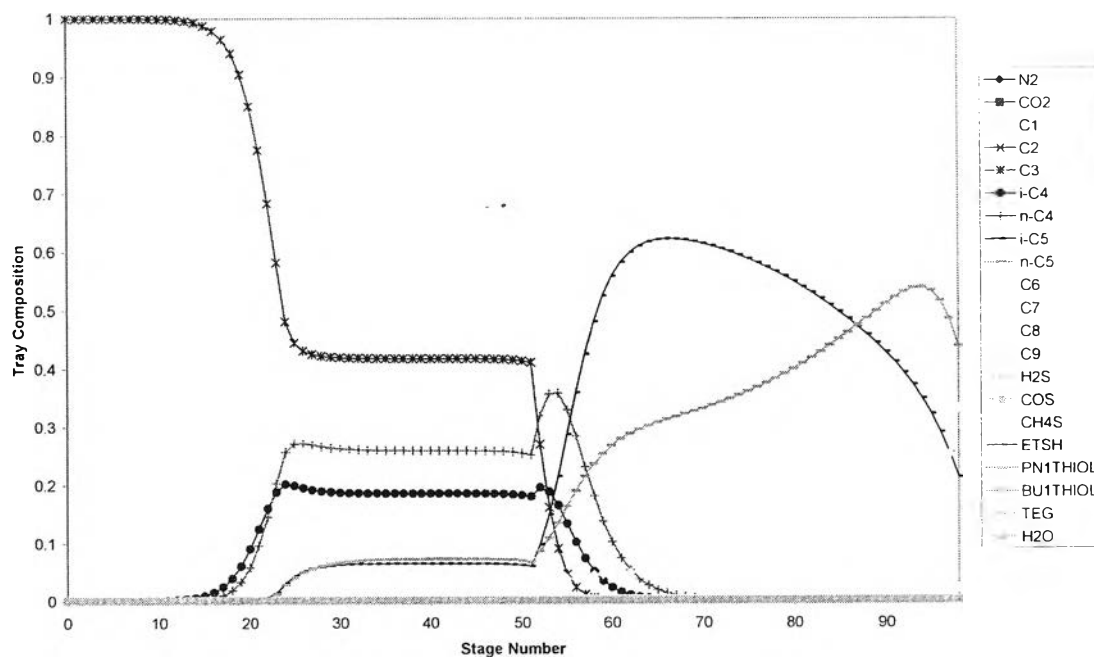


Figure 4.17(a) Depropanizer column composition profile (actual-data case).

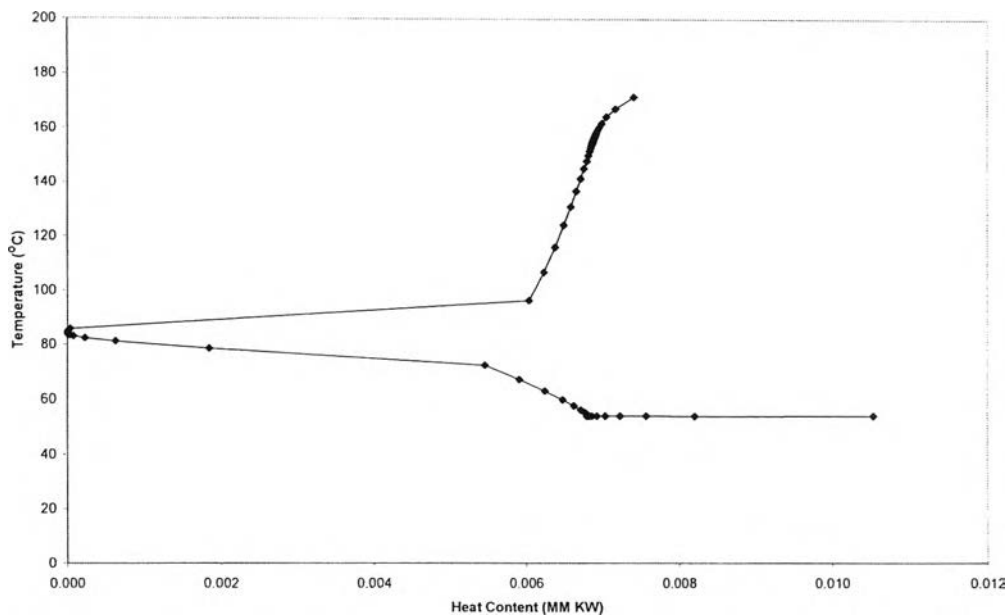


Figure 4.17(b) CGCC of the depropanizer (actual-data case).

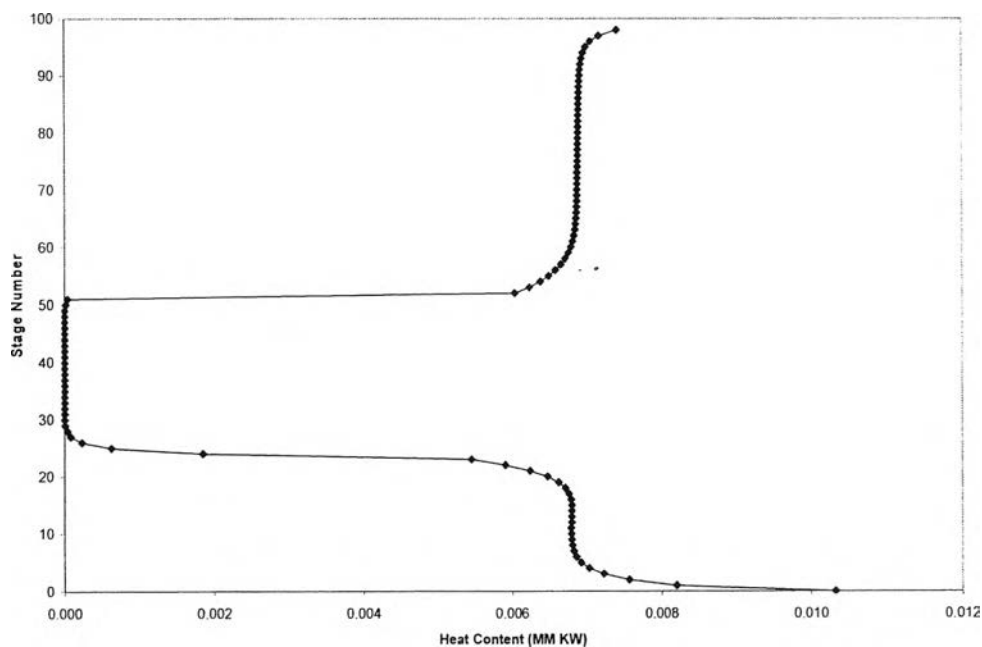


Figure 4.17(c) Stages versus enthalpy of the depropanizer (actual-data case).

Demethanizer (3503T01): The reason to not generate the CGCC of the demethanizer is similar to the design-data case; therefore, the column targeting is not appropriate to find the energy savings of the demethanizer; however, the

refrigeration system is another way to improve energy recovery for the demethanizer. Figure 4.15 shows the demethanizer column composition profile.

Deethanizer (3503T02): The CGCC of the deethanizer shown in Figure 4.16(b) gives only one pinch point at stage 12 with a tray temperature of around 33.9°C. The energy loss gap is observed, which implies an improper existing reflux ratio ($R=1.733$), which can be modified by reflux modification. The stage-enthalpy representation in Figure 4.16(c) does not show the sharp enthalpy changes near the feed position; thus, no scope of feed conditioning.

Depropanizer (3504T01): The CGCC of the depropanizer has only one pinch point at stage 49 with a tray temperature of around 84.8°C, as shown in Figure 4.17(b). There is no energy loss gap observed from the CGCC; therefore, the existing reflux ratio ($R=6.0$) might be already optimized. In Figure 4.17(c), the scope of feed preheating is observed. The sharp energy changes slightly above the feed position can be modified to reduce energy loads in a reboiler.

4.2.3.1 Sensitivity Analysis of the Columns

Before doing modifications, the column parameters, including feed stage location and reflux ratio, were studied to optimize the columns.

Sensitivity Analysis of the Deethanizer: In order to verify the optimal feed stage, the relationship between ethane purity and feed stage position was determined and the result is shown in Figure 4.18. It can be seen that the ethane purity will be maximum at 0.9868 when the deethanizer is fed in stage 11-25. The deethanizer feed is located at tray number 12, where the optimal range is. Moreover, the ethane purity will reach maximum when the reflux ratio of the deethanizer is greater than 1.689; therefore, the existing reflux ratio ($R=1.733$) can be used to get the maximum ethane purity, as shown in Figure 4.19.

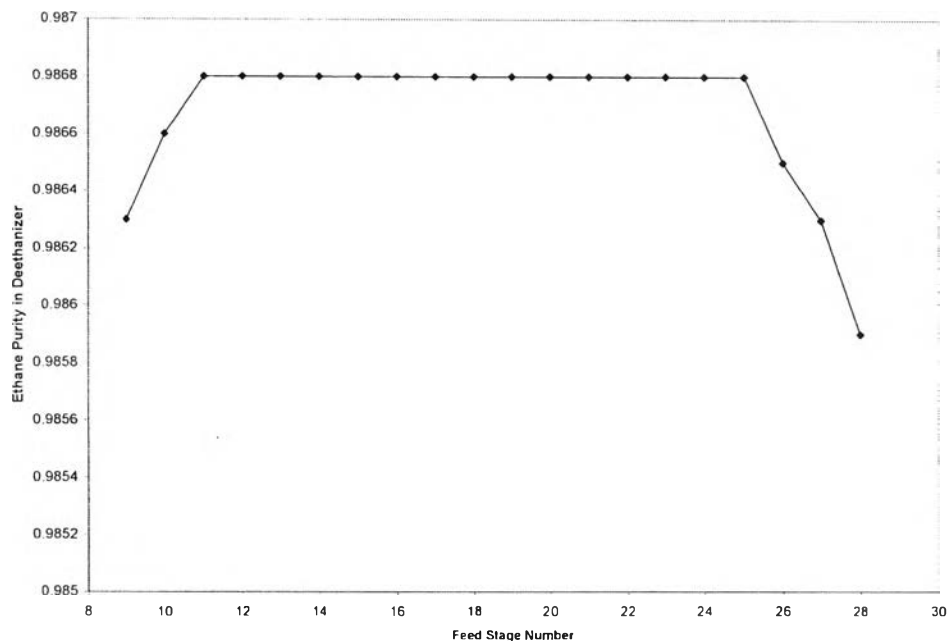


Figure 4.18 Relationship between ethane purity and feed position of the deethanizer.

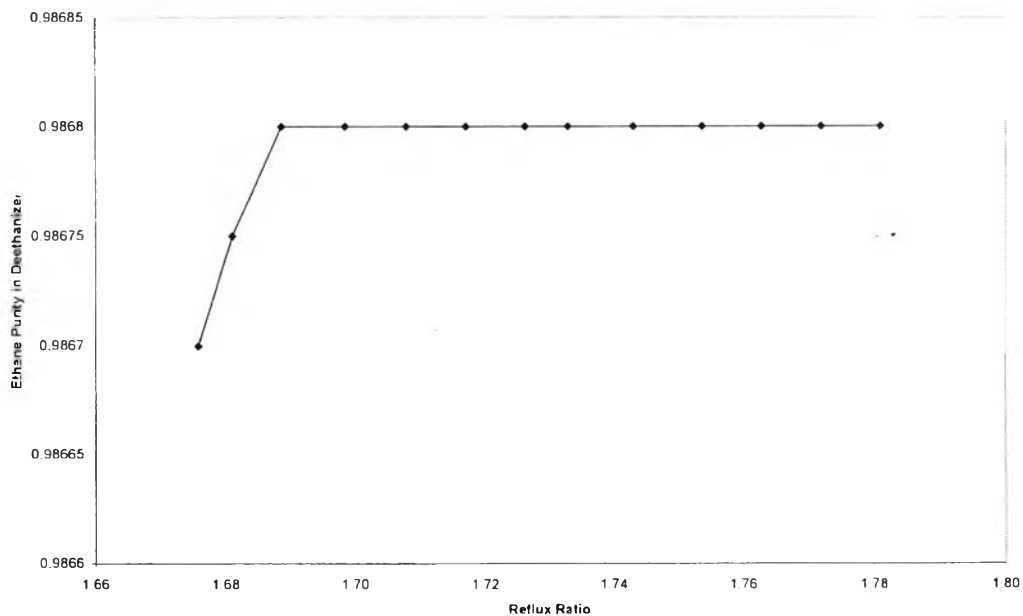


Figure 4.19 Relationship between ethane purity and reflux ratio of the deethanizer.

Sensitivity Analysis of the Depropanizer: It can be seen from Figure 4.20 that the existing feed position of the depropanizer (stage 51) was already in the optimum range to get the maximum propane purity; furthermore, the existing

reflux ratio ($R= 6.0$) can give the maximum propane purity around 0.9995 as shown in Figure 4.21.

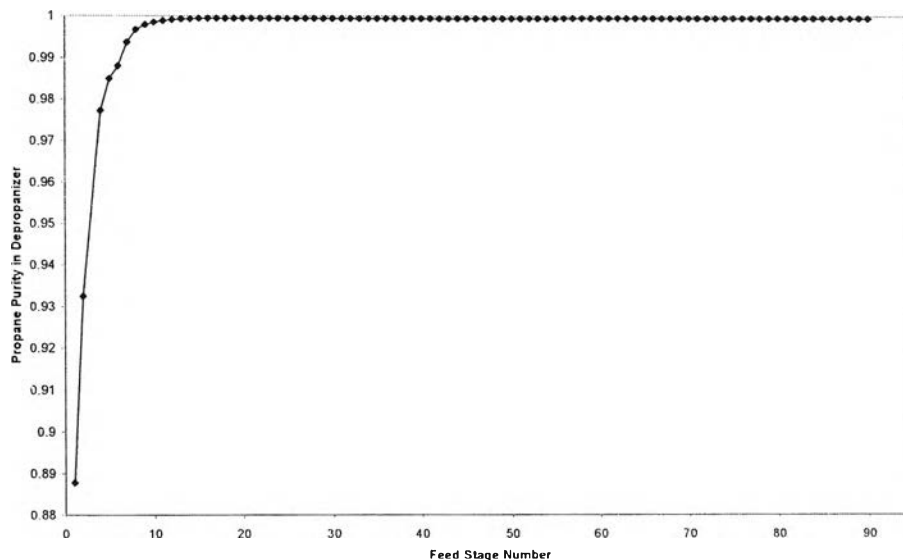


Figure 4.20 Relationship between propane purity and feed position of the depropanizer.

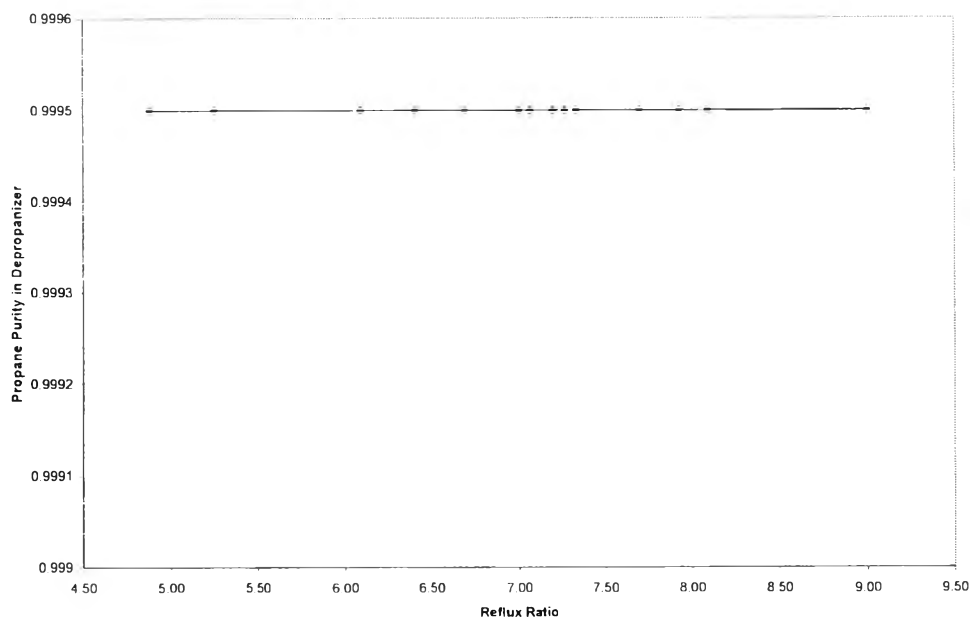


Figure 4.21 Relationship between propane purity and reflux ratio of the depropanizer.

4.2.3.2 Stand-Alone Column Modifications

For optimum performance, modifications of reflux ratio, feed conditioning (feed preheating/cooling), and side condensing/reboiling may be necessary. The priority of modification parameters of column are described in CHAPTER I. Moreover, side condensing/reboiling can be modified with Process Heat Integration.

4.2.3.2.1 Deethanizer Column Modifications

Reflux Modification: After reducing the reflux ratio, both reboiler and condenser duties are reduced (Dhole and Linnhoff, 1992), as shown in Figure 4.22. The reasonable reflux ratio is around 1.70 because this operation does not have much affect on the product specification and the product rate. However, after comparing the energy savings to other modification options; options A, B, C, D, E, and F (In this case, the process engineers want to maintain existing propane specification), this technique was not used for the deethanizer modification. The results from reflux ratio reduction on the deethanizer utility (condenser and reboiler duty) are summarized in Table 4.13. On the other hand, the effects of these reductions on product specification are also shown in Appendix D.

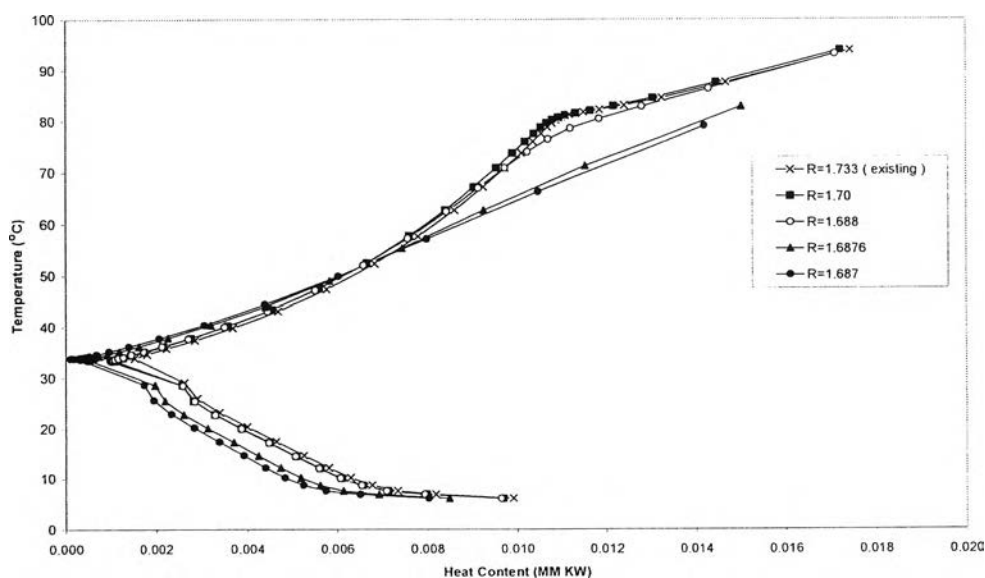


Figure 4.22 Reducing reflux ratio of the deethanizer.

Table 4.13 Results of reflux-ratio reduction of the deethanizer

| Reflux Ratio of the Deethanizer | Flow Rate (Kgmol/Hr) | | Deethanizer Utility Saving | |
|---------------------------------|----------------------|------------|----------------------------|-------|
| | Reflux | Distillate | KW | % |
| 1.733 (existing) | 3886.82 | 2242.80 | | |
| 1.70 | 3808.35 | 2240.39 | 419.00 | 1.59 |
| * 1.688 | 3767.40 | 2231.76 | 574.50 | 2.18 |
| * 1.6876 | 3480.61 | 2062.44 | 3317.90 | 12.56 |
| * 1.687 | 3357.30 | 1990.07 | 4486.60 | 16.99 |

* The products do not meet the specifications (see Appendix D).

4.2.3.2.2 Depropanizer Column Modifications

Feed Preheating: There were two modification options for feed preheating; options A and B. Option A uses a hot process stream S-100 (100.054°C) to preheat feed of the depropanizer to 90°C. Furthermore, this option also resulted in decreasing the air cooled heat exchange unit 3506E01 duty, which means lowering the cold utility consumption of the process. Option B uses a hot process stream S-99 (98.84°C) to increase the depropanizer feed to 88°C and also decrease air cooled heat exchange unit 3506E02 duty. Table 4.14 summarizes the results of feed preheating on utility saving. These two modifications had to introduce a new heat exchanger; therefore, the cost of the new heat exchanger and the energy saving would be compromised

Table 4.14 Results of feed preheating on the depropanizer

| Option | Utility Saving (KW) | | | Utility Saving (%) | | |
|--------|---------------------|---------|---------|--------------------|---------|---------|
| | Depropanizer | 3506E01 | 3506E02 | Depropanizer | 3506E01 | 3506E02 |
| A | 4000 | 4314 | | 21.2 | 35.36 | |
| B | 3180 | | 3699 | 16.85 | | 31.01 |

4.2.4 Process Heat Integration

Figure 4.23 reveals that the maximum heat recovery can be obtained from integration between the deethanizer and the heat exchanger networks of the background process by integrating a hot process stream which has a temperature above 63°C , with a new side reboiler on the deethanizer around a tray temperature of $33.9\text{-}93.9^{\circ}\text{C}$.

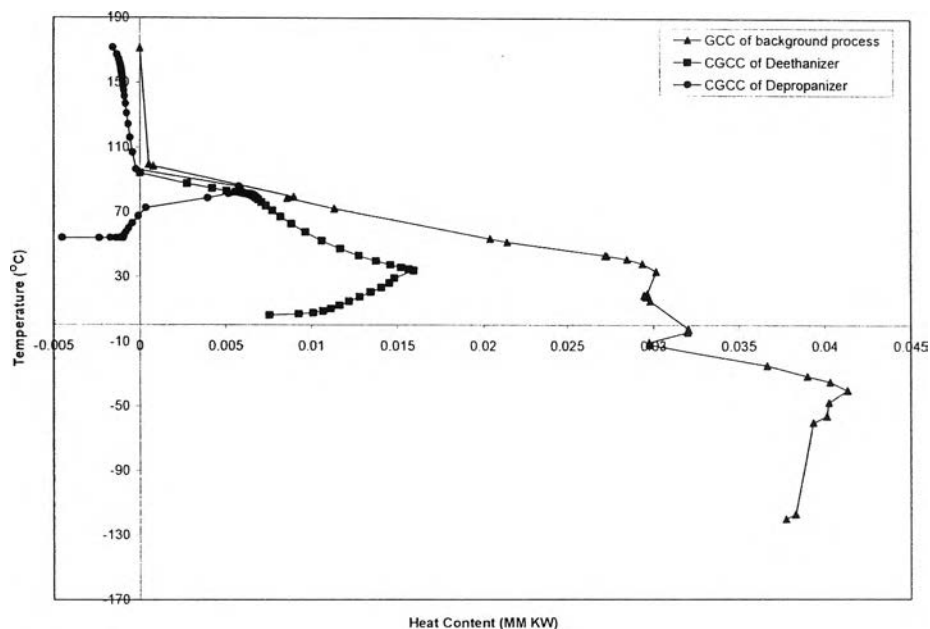


Figure 4.23 Process heat integration of the actual-data case.

After investigation, two hot processes streams (S-100 and S-99) at air cooled heat exchange units 3506E01 and 3506E02, respectively, were selected to recover energy. Option C integrates the hot process stream S-100 with a new side reboiler on tray number 39 of the deethanizer and a side-draw of around 755 kgmol/hr at this stage. This option results in hot utility and cold utility savings at the main reboiler of the deethnaizer and air cooled heat exchange unit 3506E01, respectively. Option D uses the hot process stream S-99 with a side-draw of around 597 kgmol/hr from the deethanizer and can save duty in both the main reboiler of the deethnaizer and air cooled heat exchange unit 3506E02. The results of these two options, after adding a side reboiler on the deethanizer, are summarized in Tables 4.15 and 4.16.

Table 4.15 Saving-energy after adding a side reboiler on the deethanizer (Option C)

| Modification Option | Utility Saving (KW) | | Utility Saving (%) | |
|------------------------|---------------------|---------|--------------------|---------|
| | Deethanizer | 3506E01 | Deethanizer | 3506E01 |
| C | 2313 | 2326 | 8.76 | 19.07 |

Table 4.16 Saving-energy after adding a side reboiler on the deethanizer (Option D)

| Modification Option | Utility Saving (KW) | | Utility Saving (%) | |
|------------------------|---------------------|---------|--------------------|---------|
| | Deethanizer | 3506E02 | Deethanizer | 3506E02 |
| D | 1813 | 1838 | 6.88 | 15.41 |

4.2.5 Summary of Modification Designs

The modification designs of the GSP5 can be options A, B, C, or D. Furthermore, the alternative modification designs, options E and F, can be obtained by combining options A and D and options B and C, respectively, as represented in Figure 4.24. Finally, Tables 4.17 and 4.18 conclude the overall process utility saving and an investment cost (excluding a revamp of air cooled heat exchange unit 3504E03). Moreover, the economical evaluations for various modification options with revamp studies are discussed in the section 4.2.6 (UA Analysis for Various Modification Options). The details of the cost calculation and the flow sheet of the modification options are represented in Appendices E and F.

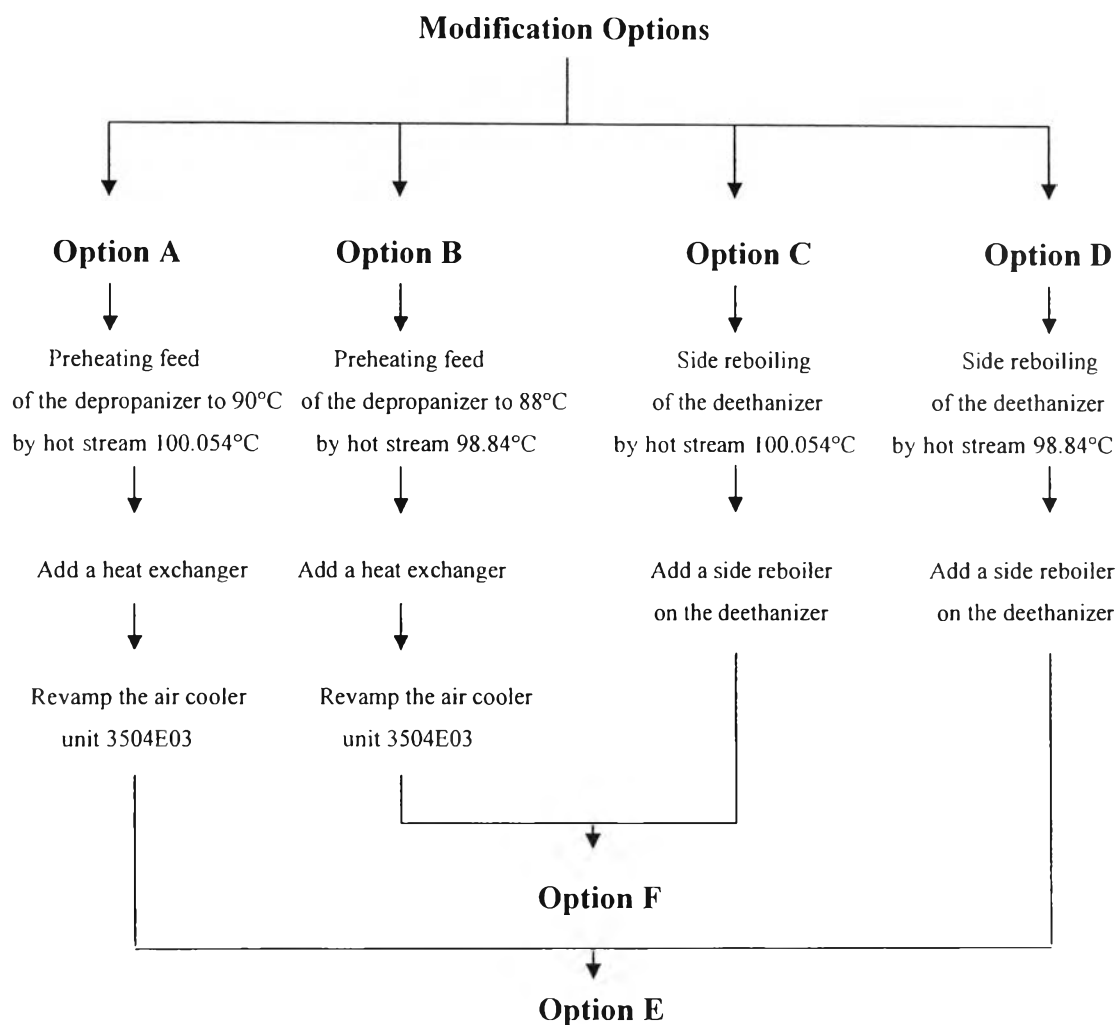


Figure 4.24 Summary of various modification options for the GSP5.

Table 4.17 Overall process utility saving for various modification options

| Modification Option | Overall Process Utility Saving | |
|---------------------|--------------------------------|-------|
| | KW | % |
| A | 8314.0 | 9.47 |
| B | 6871.1 | 7.83 |
| C | 4648.0 | 5.29 |
| D | 3660.0 | 4.17 |
| E | 11345.5 | 12.92 |
| F | 11694.1 | 13.32 |

Table 4.18 Summary of investment for various modification options (excluding the revamp studies)

| Modification Option | New Heat Exchanger Area (m ²) | Investment Cost (US\$) |
|---------------------|---|------------------------|
| A | 1365.30 | 1922869.96 |
| B | 945.23 | 1542178.97 |
| C | 2012.08 | 2426603.28 |
| D | 2010.92 | 2425764.24 |
| E | Approximately (Option A + Option D) | |
| F | Approximately (Option B + Option C) | |

4.2.6 U.A. Analysis for Various Modification Options (Revamp Studies)

Table 4.19 summarizes UA values of heat exchangers for various modification options. After modifying, options C and D allowed all heat exchangers to remain un-modified, yet options A, B, E, and F had to adapt air cooled heat exchange unit 3504E03 (the condenser of the depropanizer) because their total areas are larger than the existing ones. There are three techniques to solve this problem; by increasing fan speed, by adding the area into the heat exchange unit 3504E03, or by introducing a new heat exchanger which has the same added area. In this work, the problem can be overcome by using the last technique; therefore, an extra-investment cost should be considered for selecting retrofit options. The added area of the air cooled heat exchange unit 350403 for options A, B, E, and F are shown in Table 4.20. Furthermore, the economical evaluations for various modification options (including a revamp of air cooled heat exchange unit 3504E03) are summarized in Table 4.21

Table 4.19 UA values of each heat exchanger for various modification options

| Heat Exchanger | UA (KW/K) | | | | | | |
|----------------|-----------|-------------------------|-------------------------|----------|----------|-------------------------|-------------------------|
| | Existing | Option A | Option B | Option C | Option D | Option E | Option F |
| 3504E01 | 45.19 | 41.63 | 44.49 | 40.57 | 40.57 | 40.20 | 40.03 |
| 3504E03 | 2705.07 | 2767.83 (MOD) | 2809.68 (MOD) | 2705.40 | 2706.04 | 2836.93 (MOD) | 2776.68 (MOD) |
| 3504E04 | 144.15 | 145.68 | 144.29 | 144.20 | 144.20 | 144.32 | 144.44 |
| 3504E05 | 17.71 | 16.45 | 17.47 | 17.71 | 17.71 | 17.55 | 17.46 |
| 3504E06 | 185.75 | 185.75 | 180.52 | 186.24 | 186.48 | 180.74 | 181.38 |
| 3506E01 | 838.75 | 624.77 | 838.58 | 718.72 | 838.76 | 624.77 | 718.72 |
| 3506E02 | 830.31 | 829.94 | 742.59 | 830.33 | 790.31 | 790.31 | 742.59 |

Table 4.20 Extra-investment of air cooled heat exchange unit 3504E03 after doing UA analysis

| Modification Option | Added Area (m ²) | Added Area (%) | Investment Cost (US\$) |
|---------------------|------------------------------|----------------|------------------------|
| Option A | 103.62 | 2.32 | 26728.99 |
| Option B | 172.72 | 3.87 | 44553.85 |
| Option E | 217.71 | 4.87 | 56158.55 |
| Option F | 118.23 | 2.65 | 30497.71 |

Table 4.21 Economical evaluation for various modification options (including a revamp of air cooled heat exchange unit 3504E03)

| Modification Option | Utility Cost Saving (US\$/Yr) | Investment Cost (US\$) | Payback Period (Yr) |
|---------------------|-------------------------------|------------------------|---------------------|
| A | 4339327.91 | 1949598.95 | 0.45 |
| B | 3650661.57 | 1586732.82 | 0.43 |
| C | 2388736.11 | 2426603.28 | 1.02 |
| D | 1888047.06 | 2425764.24 | 1.28 |
| E | 6086129.45 | 4404792.75 | 0.72 |
| F | 6125989.12 | 3999279.95 | 0.65 |